

# A BOOTSTRAP PERSPECTIVE ON STOCHASTIC GRADIENT DESCENT

000  
001  
002  
003  
004  
005  
006  
007  
008  
009  
010  
011  
012  
013  
014  
015  
016  
017  
018  
019  
020  
021  
022  
023  
024  
025  
026  
027  
028  
029  
030  
031  
032  
033  
034  
035  
036  
037  
038  
039  
040  
041  
042  
043  
044  
045  
046  
047  
048  
049  
050  
051  
052  
053  
Anonymous authors  
Paper under double-blind review

## ABSTRACT

Machine learning models trained with *stochastic* gradient descent (SGD) can generalize better than those trained with deterministic gradient descent (GD). In this work, we study SGD’s impact on generalization through the lens of the statistical bootstrap: SGD uses gradient variability under batch sampling as a proxy for solution variability under the randomness of the data collection process. We use empirical results and theoretical analysis to substantiate this claim. In idealized experiments on empirical risk minimization, we show that SGD is drawn to parameter choices that are robust under resampling and thus avoids spurious solutions even if they lie in wider and deeper minima of the training loss. We prove rigorously that by implicitly regularizing the trace of the gradient covariance matrix, SGD controls the algorithmic variability. This regularization leads to solutions that are less sensitive to sampling noise, thereby improving generalization. Numerical experiments on neural network training show that explicitly incorporating the estimate of the algorithmic variability as a regularizer improves test performance. This fact supports our claim that bootstrap estimation underpins SGD’s generalization advantages.

## 1 INTRODUCTION

### 1.1 BACKGROUND

Modern machine learning models are typically overparameterized and/or non-convex, resulting in many parameter choices that achieve good training performance. However, the test performance of these parameter choices can be vastly different, making the training algorithm an important element of generalization. Notably, SGD tends to find training loss minima that generalize better on test data than GD (Zhang et al., 2016). This work aims to clarify the mechanism underlying this phenomenon.

Some studies explain this phenomenon by suggesting that the noise in SGD induces it toward flatter minima in the loss landscape, which they argue are associated with better generalization performance (Keskar et al., 2016; Yang et al., 2023; Wu & Su, 2023). However, this explanation is undermined by the lack of invariance under function reparameterization (Dinh et al., 2017; Andriushchenko et al., 2023). Another line of work provides stability-based bounds on the generalization gap (Bousquet et al., 2020; Zhou et al., 2022). These approaches usually assume uniform smoothness of the loss function, which can be overly loose in certain regions for complex loss functions. Consequently, these bounds may be trivial at solutions to which the algorithms converge. To address these limitations, we introduce a bootstrap estimation perspective to understand the generalization advantage of SGD.

### 1.2 OUR CONTRIBUTIONS

We propose that the mini-batch gradient variability in SGD acts as a bootstrap estimate of the solution’s sensitivity to resampling, which we term algorithmic variability, and SGD implicitly regularizes this bootstrap estimate to enhance generalization. This perspective motivates the design of new regularizers that can further improve generalization. Our main contributions are:

- We conduct an idealized experiment of function optimization to show that the gradient variability plays an important role in the generalization performance of SGD. More specifically, the data-dependent gradient noise steers SGD away from regions with high variability.

- Under certain assumptions, we derive an approximation of the expected generalization gap, which is determined by the solution’s Hessian matrix and the algorithmic variability with respect to sampling noise. We further derive an approximate upper bound on the algorithmic variability, which consists of two components. We propose that SGD utilizes the accumulated gradient variability as a bootstrap estimate of the first component of the algorithmic variability bound and implicitly regularizes it, thereby enhancing generalization.
- We conduct numerical experiments on SGD with explicit regularizers corresponding to estimates of the two components of the algorithmic variability bound. The results demonstrate that both components are essential for reducing test losses and that regularizers based on these estimates can be effectively applied in neural network training. To the best of our knowledge, no prior work has employed the second component of the algorithmic variability bound as a regularizer.

### 1.3 PAPER OUTLINE

Section 2 introduces the key concepts used in this work and conducts an idealized experiment to illustrate the importance of data-dependent gradient noise in helping SGD generalize better. Section 3 discusses the main theoretical conclusions of this work. We first prove that the expected generalization gap depends on the algorithmic variability. Then, we propose that SGD implicitly regularizes the bootstrap estimate of a bound on the algorithmic variability to enhance generalization. Section 4 provides experimental results that support our analysis and show that estimates of the algorithmic variability bound can be used as explicit regularizers. Section 5 reviews related work. Section 6 concludes this paper.

## 2 PRELIMINARIES

### 2.1 EMPIRICAL RISK MINIMIZATION AND GENERALIZATION GAP

Because the population distribution is inaccessible, the training loss, also called the empirical risk, is minimized as a surrogate for the population loss. The difference between the training loss and the population loss, known as the generalization gap, quantifies how well the model generalizes.

### 2.2 STOCHASTIC GRADIENT DESCENT

Gradient-based methods are widely employed for optimizing objective functions in machine learning. Unlike standard GD, which updates the model parameters with the gradient of the entire training set, SGD uses the gradient of a mini-batch randomly sampled from the training set at each iteration. The sampling noise in SGD can be captured by a gradient noise term in its update rule. Initially introduced to improve scalability with large datasets, SGD has demonstrated superior generalization performance with various models and tasks compared with GD. We will show in Section 2.4 that the data-dependent noise is essential in pushing SGD out of minima that generalize poorly.

### 2.3 BOOTSTRAP ESTIMATION

Given an estimator, we may wish to know how it would have differed over different samples. Bootstrap estimation measures this variability by treating the training set as an empirical distribution and evaluating the variability of the estimate over subsamples drawn from it.

The gradient variability of SGD evaluates how much the gradient changes with different samples from the training set. This connection motivates our explanation of SGD’s generalization behavior through the lens of bootstrap estimation.

### 2.4 AN IDEALIZED EXPERIMENT

We use an idealized experiment to show that the sampling noise, or equivalently, the gradient noise, can induce SGD to converge to solutions with better generalization compared to GD. To show the importance of the data-dependent noise, we also conduct experiments with NoisyGD, which adds data-independent Gaussian noise to each GD update.

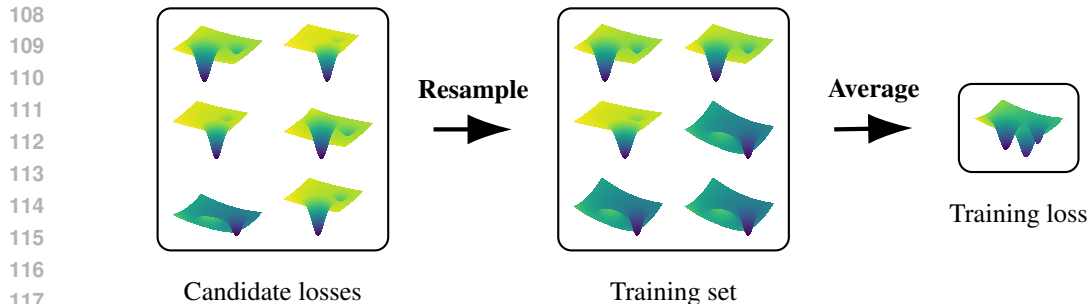


Figure 1: Construction of loss functions in the idealized experiment.

121 We run GD, SGD, and NoisyGD to optimize two-dimensional objective functions with the same  
122 initializations and hyperparameters. Each objective function is constructed by sampling 30 functions  
123 with replacement from a set of 30 candidate functions and averaging them, as illustrated in Figure  
124 1. For each algorithm, we report the mean test loss over 100 runs with different initializations. The  
125 detailed experimental setup is in Appendix A.1.

Table 1: Average test losses of algorithms in the idealized experiment.

ALGORITHM	TEST LOSS
GD	$13.99 \pm 1.67$
SGD	$5.33 \pm 1.73$
NoisyGD	$11.09 \pm 1.71$

134 Random sampling can produce training sets with samples deviating substantially from other samples  
135 in the population. These deviations yield spurious minima in the training loss landscape that fit the  
136 training data well but generalize poorly. Avoiding such spurious minima is crucial for generalization.

137 Figure 2 reports the experimental results. The population and training loss heat maps show a better-  
138 generalizing minimum at (7, 7) and a spurious minimum at (7, 1). Among the three algorithms,  
139 SGD spends most of the training time in regions where the trace of the gradient covariance matrix  
140 is small. Even though the spurious minimum is deeper, broader, and has smaller gradient norms  
141 in its neighborhood than the better-generalizing minimum in the training loss landscape, SGD still  
142 converges to the latter owing to its smaller variability. This observation is corroborated in Table 1,  
143 where SGD has the smallest average test loss among the algorithms. These results indicate that the  
144 data-dependent gradient noise enables SGD to avoid converging to spurious minima arising from  
145 random sampling from the population. This finding inspires the idea that SGD utilizes gradient  
146 variability to estimate the sensitivity of the solution to different training data.

### 3 THEORETICAL RESULTS

147 In Section 2.4, we show with the idealized experiment that SGD converges to solutions with small  
148 gradient variability, which generalize well to the test data. This observation raises two key questions:  
149 (1) what factor drives SGD to solutions with small gradient variability? (2) how does this reduced  
150 gradient variability improve generalization? In this section, we formally establish the connection  
151 between the gradient variability and generalization. First, under the assumptions that SGD can achieve  
152 small gradient on the training data and that replacing one training sample has only a minor impact on  
153 the solution, we show that the expected generalization gap can be decomposed into the trace of the  
154 product between the solution’s Hessian and the algorithmic variability, which measures the sensitivity  
155 of the solution to replacing a single sample in the training set. Then, we demonstrate that the gradient  
156 variability of SGD can be regarded as a bootstrap estimate of the first component of a bound on the  
157 algorithmic variability. Lastly, we show that the implicit regularizer of SGD, as characterized by  
158 Smith et al. (2021), is equivalent to regularizing gradient variability. Taken together, these points  
159 suggest that the implicit regularizer steers SGD toward solutions with smaller gradient variability,  
160 which, being a bootstrap estimate of the algorithmic variability, leads to improved generalization.  
161

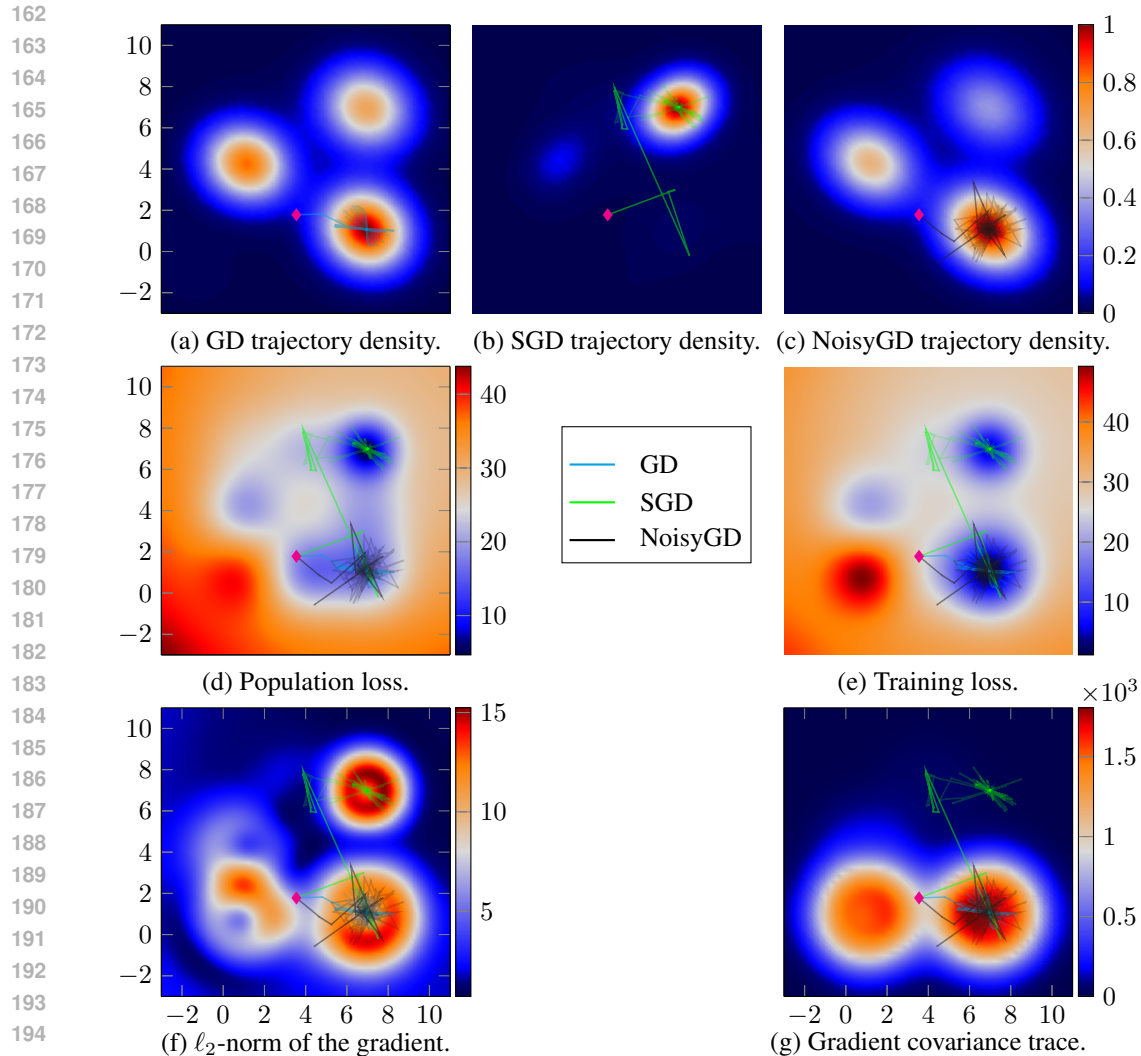


Figure 2: Heat maps of algorithm trajectory densities, population and training losses, gradient norms, and gradient covariance traces from the idealized experiment, with representative trajectories overlaid.

### 3.1 NOTATIONS

This paper focuses on supervised learning. A sample  $z = (x, y)$  consists of an input  $x \in \mathcal{X} = \mathbb{R}^d$  and a target  $y \in \mathcal{Y} = \mathbb{R}$ . Let  $S = \{z_1, z_2, \dots, z_N\}$  be a training set of size  $N$ , where the  $z_i$  are i.i.d. samples from the population distribution  $D$  on  $\mathcal{Z} = \mathcal{X} \times \mathcal{Y}$ .  $L(z; \theta)$  denotes the loss function evaluated on sample  $z$  at model parameters  $\theta$ . We slightly abuse these notations by writing the average loss on the training set  $S$  as  $L(S; \theta) = \frac{1}{N} \sum_{i=1}^N L(z_i; \theta)$  and the expected loss on the population distribution  $D$  as  $L(D; \theta) = \mathbb{E}_{z \sim D} [L(z; \theta)]$ .

For a training set  $S$ , let  $A_t(S)$  denote the solution obtained by applying SGD to  $S$  for  $t$  iterations, starting from initialization  $A_0$ . A specific SGD instantiation  $A_T$  can be represented by  $\{j_1, j_2, \dots, j_T\}$ , where  $j_t$  indicates that sample  $z_{j_t}$  in  $S$  is selected at iteration  $t$ .  $\mathbb{E}_{A_T} [f]$  takes the expectation of function  $f$  over all possible  $A_T$ , given a fixed model initialization  $A_0$  and a learning rate schedule  $\{\eta_1, \eta_2, \dots, \eta_T\}$ . We can construct a perturbed training set for  $S$  by replacing the  $i$ -th sample with a new one drawn from the population distribution:  $S^i = \{z_1, \dots, z_{i-1}, z'_i, z_{i+1}, \dots, z_N\}$ ,  $z'_i \sim D$ . Unless stated otherwise,  $\mathbb{E}_{z'_i} [f]$  denotes the expectation of function  $f$  over  $z'_i$  drawn from the population distribution  $D$ . For brevity, we define  $J(v) = vv^T$  for any vector  $v$ .

216 3.2 DECOMPOSITION OF THE EXPECTED GENERALIZATION GAP  
217218 We derive a decomposition of the expected generalization gap under the following assumptions.  
219220 **Assumption 1.** For  $S \in \mathcal{Z}^N$ , with probability  $1 - \delta_{1,T}$ , SGD obtains a solution whose batch gradient  
221  $\ell_2$ -norm is bounded by  $\epsilon_{1,T}$  after  $T$  iterations, i.e.,  
222

223 
$$\Pr(\|\nabla L(S; A_T(S))\|_2 > \epsilon_{1,T}) < \delta_{1,T}$$
  
224

225 for some  $0 < \epsilon_{1,T}, \delta_{1,T} \ll 1$ .  
226227 Multiple studies have shown that overparameterized models can interpolate training sets under  
228 suitable conditions (Richtárik & Takáć, 2020; Vaswani et al., 2019; Loizou et al., 2021). Consequently,  
229 Assumption 1 holds broadly across many machine learning problems.  
230231 **Assumption 2.** For  $S \in \mathcal{Z}^N$ , with probability  $1 - \delta_{2,T}$ , the  $\ell_2$ -norm of the deviation between the  
232 solutions obtained by running SGD for  $T$  iterations on  $S$  and its perturbed training set  $S^i$  is bounded  
233 by  $\epsilon_{2,T}$ , i.e.,  
234

235 
$$\Pr(\|A_T(S) - A_T(S^i)\|_2 > \epsilon_{2,T}) < \delta_{2,T}$$
  
236

237 for some  $0 < \epsilon_{2,T}, \delta_{2,T} \ll 1$ .  
238239 Assumption 2 concerns the solution stability under single-sample replacements and holds when the  
240 training set is sufficiently large that such replacements have a small effect.  
241242 **Lemma 1.** Consider a loss function  $L$  whose value is bounded by  $U_L$ , with batch gradient  $\ell_2$ -norm  
243 bounded by  $U_G$  and all third-order partial derivatives bounded by  $U_J$ . Assume the parameters are  
244 bounded as  $\|\theta\|_2 \leq U_F$ . If Assumptions 1 and 2 hold for  $L$ , the expected generalization gap satisfies  
245

246 
$$\mathbb{E}_{S, A_T} [L(D; A_T(S)) - L(S; A_T(S))] \quad (1)$$
  
247

248 
$$= \frac{1}{N} \sum_{i=1}^N \mathbb{E}_{S, z'_i, A_T} [L(z'_i; A_T(S))] - \frac{1}{N} \sum_{i=1}^N \mathbb{E}_{S, z'_i, A_T} [L(z'_i; A_T(S^i))] \quad (2)$$
  
249

250 
$$= \mathbb{E}_{S, A_T} \left[ \frac{1}{2} \text{Tr} \left( \nabla^2 L(S; A_T(S)) \frac{1}{N} \sum_{i=1}^N \mathbb{E}_{z'_i} [J(A_T(S^i) - A_T(S))] \right) \right] \quad (3)$$
  
251

252 
$$+ \mathcal{O}(\epsilon_{1,T} \epsilon_{2,T} + \delta_{1,T} \epsilon_{2,T} U_G + \delta_{1,T} \delta_{2,T} U_G U_F + \epsilon_{2,T}^3 U_J + \delta_{2,T} U_L). \quad (4)$$
  
253

254 Lemma 1 provides the expected generalization gap decomposition, with its proof given in Appendix  
255 B.1.  $\mathbb{E}_{S, z'_i, A_T} [L(z'_i; A_T(S))]$  denotes the expectation of  $L(z'_i; A_T(S))$  over  $S \sim D^N, z'_i \sim D$   
256 and SGD instantiations initialized at  $A_0$ . The big-O term arises from the remainder of the Taylor  
257 expansion, and its constant does not depend on the problem setting. For the second-order Taylor  
258 expansion to be accurate, it suffices that all the third-order partial derivatives in a neighborhood of the  
259 solution are bounded by the smallest eigenvalue of its Hessian, scaled by  $\epsilon_{2,T}$ . This condition may fail  
260 for degenerate solutions, but note that flat directions contribute far less to the expected generalization  
261 gap than sharp ones. Combined with the alignment between the Hessian and the gradient covariance  
262 of SGD (Wu et al., 2022), this justifies the approximation.  
263264 The decomposition depends on the solution’s Hessian and  $\frac{1}{N} \sum_{i=1}^N \mathbb{E}_{z'_i} [J(A_T(S^i) - A_T(S))]$ .  
265 We denote this latter term as the *algorithmic variability*, which measures the sensitivity of the  
266 solution to single-sample replacements in the training set. Next, we will show that SGD automatically  
267 estimates and regularizes this variability term.  
268

## 269 3.3 BOOTSTRAP ESTIMATION OF THE ALGORITHMIC VARIABILITY

270 We proceed to demonstrate that SGD uses the accumulated gradient covariance as a bootstrap  
271 estimate of part of a bound on the algorithmic variability. The analysis in this subsection relies on the  
272 data-dependent gradient noise of SGD and therefore does not extend to GD.  
273274 **Lemma 2.** Consider the case where the model is trained with SGD on the training set  $S$  for  $M$   
275 epochs, with each sample appearing exactly once in every epoch. Assume that  
276277 1. The learning rates are small, i.e., letting  $Q = \max_t \eta_t$ , we have  $Q \ll 1$ .  
278

270      2. The operator norm of  $\nabla^2 L(S; \theta)$  is uniformly bounded by a constant  $C \ll \frac{1}{Q}$ .  
 271

272      Then, the algorithmic variability can be bounded as  
 273

$$274 \quad \text{Tr} \left( \nabla^2 L(S, A_T(S)) \frac{1}{N} \sum_{i=1}^N \mathbb{E}_{z'_i} [J(A_T(S^i) - A_T(S))] \right) \quad (5)$$

$$277 \quad \leq \text{Tr} \left( \nabla^2 L(S, A_T(S)) \sum_{t=1}^T M \eta_t^2 \mathbb{E}_{z'_i} [J(\nabla L(z'_i; A_{t-1}(S)) - \nabla L(D; A_{t-1}(S)))] \right) \quad (6)$$

$$280 \quad + \text{Tr} \left( \nabla^2 L(S, A_T(S)) \sum_{t=1}^T M \eta_t^2 J(\nabla L(S_{j_t}; A_{t-1}(S)) - \nabla L(D; A_{t-1}(S))) \right) \quad (7)$$

$$283 \quad + \mathcal{O}(TQ\epsilon_{2,T}(\epsilon_{2,T}^3 U_J + \delta_{2,T} U_L U_F^3 + CQU_F) + T^2 Q^2 (\epsilon_{2,T}^3 U_J + \delta_{2,T} U_L U_F^3 + CQU_F)^2). \quad (8)$$

286      The proof of Lemma 2 is in Appendix B.2. It relies on the positive semi-definiteness of the solution's  
 287      Hessian. This condition is guaranteed since SGD avoids solutions with negative Hessian eigenvalues  
 288      almost surely (Mertikopoulos et al., 2020). Since  $Q \ll 1$ ,  $TQ = \mathcal{O}(1)$  for finite  $T$ , hence the big-O  
 289      term is bounded.

290      **Theorem 1.** Denote by  $\Sigma_B^S(\theta)$  the gradient covariance of mini-batches of size  $B$  evaluated on  
 291      dataset  $S$  at  $\theta$ . If the conditions of Lemma 2 hold,  $\theta$  lies within a compact set  $\Theta$ , and  $\nabla L(z'_i; \theta)$   
 292      is continuous with respect to  $\theta$  on  $\Theta$ , then as the training set size  $N \rightarrow \infty$ , the difference between  
 293      the accumulated population gradient covariance and the accumulated gradient covariance of SGD  
 294      converges to 0 almost surely, i.e.,

$$295 \quad \sum_{t=1}^T \mathbb{E}_{z'_i} [J(\nabla L(z'_i; A_{t-1}(S)) - \nabla L(D; A_{t-1}(S)))] - \sum_{t=1}^T B \Sigma_B^S(A_{t-1}(S)) \xrightarrow{a.s.} 0. \quad (9)$$

299      Theorem 1 is the core contribution of this work, and its proof is given in Appendix B.3. Suppose  
 300      SGD were to draw  $K$  mini-batches of size  $B$  from  $S$  at  $A_{t-1}(S)$ , the empirical gradient covariance  
 301      of these mini-batches would act as a bootstrap estimate of  $\Sigma_B^S(A_{t-1}(S))$  and converge to it as  
 302       $K \rightarrow \infty$ . Furthermore,  $B \Sigma_B^S(A_{t-1}(S))$  serves as an estimate of the population gradient covariance  
 303       $\mathbb{E}_{z'_i} [J(\nabla L(z'_i; A_{t-1}(S)) - \nabla L(D; A_{t-1}(S)))]$  and converges to it as  $N \rightarrow \infty$ . Hence, we  
 304      interpret SGD as using the accumulated mini-batch gradient covariance as a bootstrap estimation  
 305      of the accumulated population gradient covariance, which constitutes the first component of the  
 306      algorithmic variability bound in equation 6.

307      Although Theorem 1 is an asymptotic result, our experiments show that the accumulated gradient  
 308      covariance of SGD is strongly correlated with the algorithmic variability even for moderate  $N$ . We  
 309      refer to the eigenvectors corresponding to the largest eigenvalues of a matrix as its principal eigendirec-  
 310      tions. For the accumulated gradient covariance matrix to accurately estimate the accumulated  
 311      population gradient covariance, the span of the sample gradients must capture most of the principal  
 312      eigendirections of the population gradient covariance, which requires  $N$  to be at least as large as  
 313      the number of principal eigendirections of the population gradient covariance. In practice, real data  
 314      often reside in a low-dimensional subspace, which explains why the estimation is accurate even for  
 315      moderate  $N$ .

### 316      3.4 IMPLICIT REGULARIZER AND GENERALIZATION

318      We now show how SGD implicitly regularizes the first part of the algorithmic variability bound  
 319      in equation 6, thereby enhancing generalization. Smith et al. (2021) show that when  
 320      resampling mini-batches of size  $B$  without replacement, SGD implicitly regularizes the mean  
 321      squared Euclidean distance between the sample gradients and the batch gradient,  $\Gamma(\theta) =$   
 322       $\frac{1}{N} \sum_{i=1}^N \|\nabla L(z_i; \theta) - \nabla L(S; \theta)\|_2^2$ , with implicit regularizer  $\frac{N-B}{N-1} \frac{\Gamma(\theta)}{B}$ . Analogously, when re-  
 323      sampling with replacement from  $S$ , SGD implicitly regularizes  $\frac{\Gamma(\theta)}{B}$ . By algebraic manipulation, we

324 show that this quantity equals the trace of the mini-batch gradient covariance:  
 325

$$326 \quad \text{Tr}(\Sigma_B^S(\theta)) = \text{Tr}\left(\frac{\sum_{i=1}^N J(\nabla L(z_i; \theta) - \nabla L(S; \theta))}{BN}\right) = \frac{\sum_{i=1}^N \|\nabla L(z_i; \theta) - \nabla L(S; \theta)\|_2^2}{BN}. \\ 327 \\ 328 \\ 329$$

330 This implicit regularizer of SGD reduces the trace of the gradient covariance during training, thereby  
 331 controlling the algorithmic variability. Since the expected generalization gap depends on the algorithmic  
 332 variability, this implicit regularizer enables SGD to generalize better.  
 333

334 The second component of the algorithmic variability bound in equation 7 is neither estimated nor  
 335 regularized by SGD. Analogous to the bootstrap estimation in Theorem 1, we introduce a plug-in  
 336 estimator of this term as an explicit regularizer. For set  $S$ , at iteration  $t$ , we define *regularizer 1* as  
 337

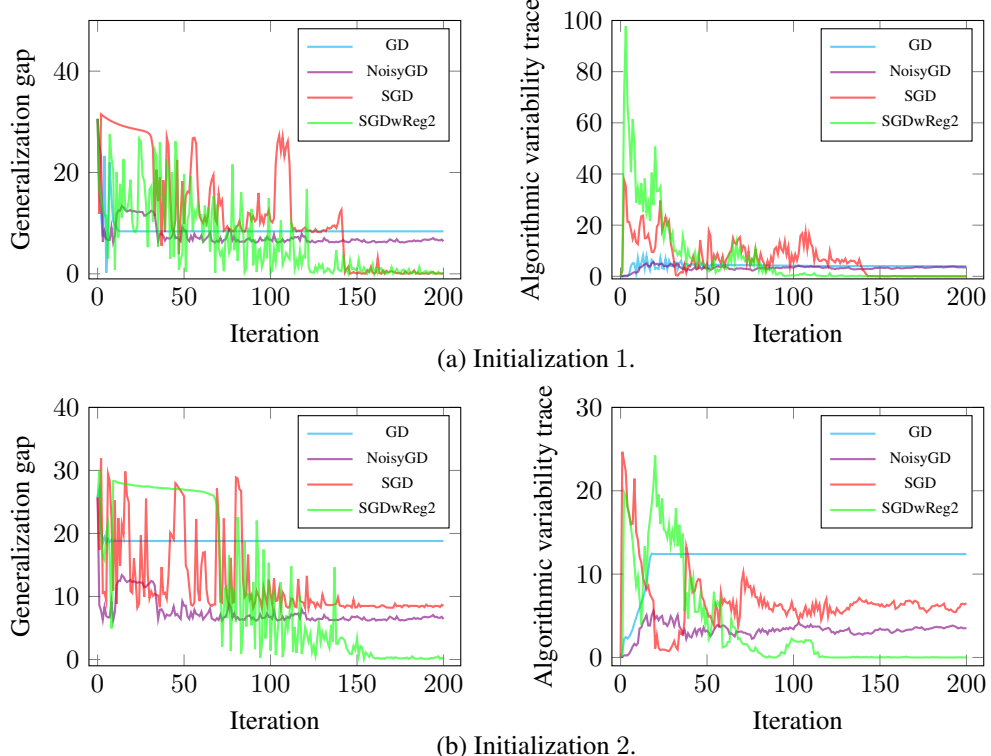
$$338 \quad \text{Reg1} = \lambda_1 \frac{1}{N} \sum_{i=1}^N \|\nabla L(z_i; A_{t-1}(S)) - \nabla L(S; A_{t-1}(S))\|_2^2 \\ 339 \\ 340$$

and *regularizer 2* as

$$341 \quad \text{Reg2} = \lambda_2 \|\nabla L(S_{j_t}; A_{t-1}(S)) - \nabla L(S; A_{t-1}(S))\|_2^2, \\ 342$$

343 with  $\lambda_1$  and  $\lambda_2$  denoting their respective strengths. These two regularizers correspond to estimates of  
 344 the two components of the algorithmic variability bound. We evaluate the impact of these regularizers  
 345 on generalization with numerical experiments in the following sections.  
 346

### 3.5 EMPIRICAL VALIDATION

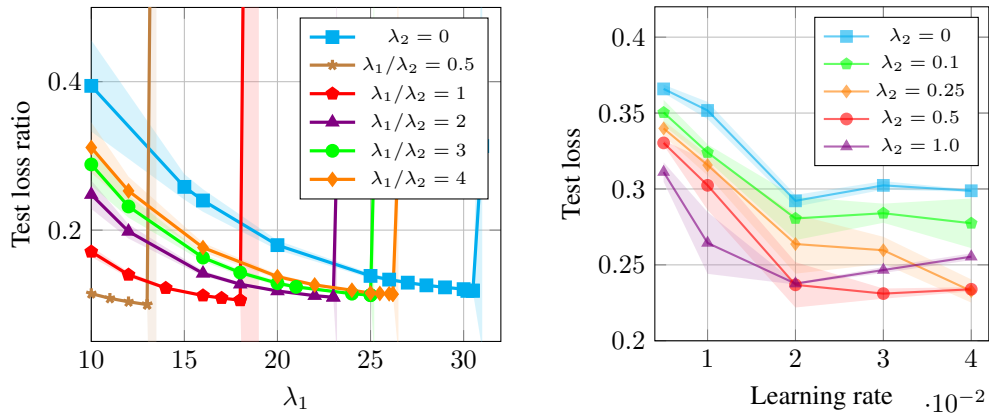


374 Figure 3: Trajectories of the generalization gap and the algorithmic variability trace versus iteration  
 375 for GD, SGD, NoisyGD, and SGDwReg2, shown for two initializations in the idealized experiment.  
 376

377 We extend the idealized experiment in Section 2.4 to illustrate the relationship between algorithmic  
 378 variability and generalization gap. In addition to the three algorithms considered above, we evaluate  
 379

378 SGDwReg2, which incorporates regularizer 2 into SGD. Figure 3 reports the trajectories of the  
 379 generalization gap and the algorithmic variability trace under two different initializations. We observe  
 380 that sharp decreases in the algorithmic variability trace coincide with reductions in the generalization  
 381 gap, and algorithms ending with smaller algorithmic variability traces exhibit smaller generalization  
 382 gaps. GD and NoisyGD have no control over the algorithmic variability, and we observe they end with  
 383 larger variability trace and generalization gap in most experiments. We deliberately choose one case  
 384 where SGD has poor generalization as Initialization 2. Notably, while SGD performs poorly under  
 385 initialization 2, SGDwReg2 consistently reduces the algorithmic variability trace and achieves good  
 386 generalization. These results align with our analysis above: while SGD only implicitly regularizes the  
 387 first component of the algorithmic variability bound, incorporating regularizer 2 enables SGDwReg2  
 388 to regularize the full bound.

## 389 4 NUMERICAL EXPERIMENTS



406 Figure 4: Average test loss ratios of SGD with reg-  
 407 ularizers 1 and 2 relative to the vanilla SGD bench-  
 408 marks. Shaded areas represent standard devia-  
 409 tions of the test loss ratios across different initializa-  
 410 tions.

406 Figure 5: Average test losses of SGD with reg-  
 407 ularizer 2. Shaded areas represent standard  
 408 deviations across three runs with different ran-  
 409 dom seeds.

### 412 4.1 SPARSE REGRESSION WITH DIAGONAL LINEAR NETWORKS

414 To evaluate the impact of regularizers 1 and 2 on generalization with moderately large training sets,  
 415 we conduct experiments on sparse regression. We incorporate both regularizers 1 and 2 into SGD, for  
 416 different fixed values of the relative strength ratio  $\frac{\lambda_1}{\lambda_2}$ , and compare their performance with that of the  
 417 vanilla SGD benchmark. The model we use is the diagonal linear network (DLN), parameterized as  
 418  $\theta = (\theta_a, \theta_b) \in \mathbb{R}^{2d}$ . This model represents the function  $f(x; \theta) = \langle \theta_a \odot \theta_b, x \rangle$ , where  $\odot$  denotes the  
 419 element-wise multiplication. Despite its simplicity, the DLN is overparameterized and provides the  
 420 non-convexity we seek (Pesme et al., 2021). We run the algorithms to minimize the mean squared  
 421 error of the training sets, which consist of 40 samples. The detailed experimental setup is in Appendix  
 422 A.2.

423 While different initializations strongly impact the test loss, the test loss ratios between different  
 424 algorithms starting from the same initialization remain stable. Therefore, for each training set and  
 425 initialization combination, we use the test loss of the vanilla SGD for that setting as the benchmark.  
 426 The performance of each algorithm is evaluated by the ratios between its test loss and this benchmark.

427 Figure 4 shows that most test loss ratios fall below 1, indicating that incorporating explicit regularizers  
 428 to SGD improves the average test loss of the solution. Within certain thresholds, increasing the  
 429 regularization strength reduces the test loss. Notably, incorporating regularizer 2 can further reduce  
 430 the test loss. Across the experimental settings, smaller relative strength ratios correspond to better  
 431 generalization performance. Compared to the  $\lambda_2 = 0$  curve, the setting  $\frac{\lambda_1}{\lambda_2} = 0.5$  reduces the best  
 432 test loss by 14%. These observations demonstrate that these regularizers improve generalization

432 for moderately large training sets. Moreover, consistent with our analysis in Section 3, while SGD  
 433 only implicitly regularizes the first component of the algorithmic variability bound to help the model  
 434 generalize, the best performance is achieved when both regularizers 1 and 2 are incorporated, thereby  
 435 regularizing the full algorithmic variability bound.

## 437 4.2 DEEP NEURAL NETWORKS

438 To evaluate the effectiveness of the proposed regularizers in practical deep neural network training,  
 439 we train a convolutional neural network (CNN) on the FashionMNIST dataset (Xiao et al., 2017).  
 440 We use SGD with weight decay regularization as a benchmark. Owing to computational budget  
 441 constraints, we incorporate only regularizer 2 and omit the batch gradient term in it. The detailed  
 442 experimental setup is in Appendix A.3.

443 Figure 5 compares the performance of different regularization strengths and the benchmark, repre-  
 444 sented by the  $\lambda_2 = 0$  curve. Overall, the average test loss decreases when we explicitly incorporate  
 445 regularizer 2. For small regularization strengths, we observe consistent improvements over the  
 446 benchmark. At larger regularization strengths, regularizer 2 yields better performance under small  
 447 learning rates, but it also carries the risk of degrading test performance as the learning rate increases.  
 448 These results demonstrate that an appropriately tuned regularizer 2 improves generalization.

## 451 4.3 COMPUTATIONAL OVERHEAD OF REGULARIZERS

452 One potential concern regarding the proposed regularizers is that both involve the batch gradient  
 453  $\nabla L(S; A_{t-1}(S))$ , and computing this term can incur large computation overhead. In practice, we  
 454 can use approximation of the batch gradient when implementing the regularizers. For instance,  
 455 the average of the previous  $k$  mini-batch gradients can be used as an approximation to the batch  
 456 gradient when the learning rate is not too large. In the experiment of Section 4.2, we omit the batch  
 457 gradient term in regularizer 2 completely because the magnitude of the batch gradient becomes much  
 458 smaller than that of most of the mini-batches quickly. In this case, the training time of SGDwReg is  
 459 approximately 2.2 times of SGD.

## 461 5 RELATED WORK

462 **Solution sharpness perspective.** Many studies try to explain the generalization behavior of SGD  
 463 from the perspective of solution sharpness. Keskar et al. (2016) show that the generalization drop  
 464 of the model is caused by the sharp minimizer it converges to when using large batches. Yang et al.  
 465 (2023); Wu & Su (2023) attribute the good generalization of a solution to its low sharpness. Moreover,  
 466 Ma & Ying (2021); Wu et al. (2022); Ibayashi & Imaizumi (2021) show that stochasticity in SGD  
 467 leads to solutions with low sharpness without explicit regularization.

468 However, these sharpness-based explanations suffer from the lack of invariance under repara-  
 469 meterization (Andriushchenko et al., 2023). Different parameterizations of the same function can  
 470 yield drastically different sharpness values. This fact undermines the claim that the generalization  
 471 performance of a function is directly correlated with its sharpness. Our perspective is related to  
 472 the sharpness views in that the expected generalization gap decomposition involves the solution’s  
 473 Hessian, but crucially differs from them because it considers the entire training trajectory. Since  
 474 reparameterization alters the training dynamics and can lead to different solutions, our perspective is  
 475 not subject to invariance issues.

476 **Algorithmic stability perspective.** Another line of work connects generalization to algorithmic  
 477 stability. Bousquet & Elisseeff (2002) and Elisseeff et al. (2005) define different kinds of stability  
 478 and lay the foundation for this branch of work. Shalev-Shwartz et al. (2010) explore the connection  
 479 between learnability and stability of empirical risk minimization. Recent works in this area include  
 480 high-probability bounds (Feldman & Vondrak, 2019), hypothesis set stability (Foster et al., 2019),  
 481 and uniformly stable algorithms (Bousquet et al., 2020). Regarding the generalization gap, Zhou  
 482 et al. (2022) give a generalization gap bound based on the gradient variability on the training set,  
 483 and Thomas et al. (2020) propose an estimation of the generalization gap based on the Hessian and  
 484 gradient covariance at the solution evaluated on the population distribution.

486 Prior stability analyses typically yield worst-case generalization bounds under uniform smoothness  
 487 assumptions, which can be overly conservative in highly non-convex settings. In contrast, our  
 488 decomposition of the expected generalization gap is Hessian-weighted and evaluated at the solutions,  
 489 thereby capturing the local curvature in regions of the loss landscape that the algorithm actually  
 490 reaches. Free from uniform smoothness bounds, this framework enables us to isolate the impact  
 491 of algorithmic variability and identify SGD’s implicit regularization on the bootstrap estimate of  
 492 algorithmic variability as the mechanism underlying its generalization advantage.  
 493

## 6 CONCLUSION

496 We provide an explanation of the generalization advantage of SGD based on a bootstrap estimation  
 497 of the algorithmic variability. Specifically, we demonstrate that SGD implicitly regularizes the trace  
 498 of the gradient covariance matrix, which serves as a bootstrap estimate of part of the algorithmic  
 499 variability bound. This regularization guides SGD toward solutions that are robust to sampling  
 500 noise, thereby enhancing generalization performance. While our theoretical analysis relies on  
 501 specific assumptions on problem settings, numerical experiments in both synthetic and real-world  
 502 settings show that our claims extend to broader settings. The experimental results demonstrate that  
 503 incorporating the bootstrap estimates as explicit regularizers can effectively improve generalization  
 504 in practice. These findings underscore the central role of the algorithmic variability in generalization  
 505 and offer new insights into designing new regularizers to enhance generalization. An important open  
 506 problem is whether the optimal regularization strength can be estimated from the training data or  
 507 automatically tuned during training.  
 508

## REPRODUCIBILITY STATEMENT

511 The detailed experimental setups for the idealized experiment, the DLN experiment, and the CNN  
 512 experiment are given in Appendix A.1, A.2, and A.3, respectively. Complete proofs for Lemma  
 513 1, Lemma 2, and Theorem 1 are given in Appendix B.1, B.2, and B.3. The source code for all  
 514 experiments conducted in this work is included in the zipped supplementary materials.  
 515

## REFERENCES

517 Maksym Andriushchenko, Francesco Croce, Maximilian Müller, Matthias Hein, and Nicolas Flam-  
 518 marion. A modern look at the relationship between sharpness and generalization, 2023. URL  
 519 <https://arxiv.org/abs/2302.07011>.  
 520

521 Olivier Bousquet and André Elisseeff. Stability and generalization. *J. Mach. Learn. Res.*,  
 522 2:499–526, 2002. URL <http://dblp.uni-trier.de/db/journals/jmlr/jmlr2.html#BousquetE02>.  
 523

524 Olivier Bousquet, Yegor Klochkov, and Nikita Zhivotovskiy. Sharper bounds for uniformly stable  
 525 algorithms. In *Conference on Learning Theory*, pp. 610–626. PMLR, 2020.  
 526

527 Laurent Dinh, Razvan Pascanu, Samy Bengio, and Yoshua Bengio. Sharp minima can generalize for  
 528 deep nets. In *International Conference on Machine Learning*, pp. 1019–1028. PMLR, 2017.  
 529

530 Andre Elisseeff, Theodoros Evgeniou, Massimiliano Pontil, and Leslie Pack Kaelbling. Stability of  
 531 randomized learning algorithms. *Journal of Machine Learning Research*, 6(1), 2005.  
 532

533 Vitaly Feldman and Jan Vondrak. High probability generalization bounds for uniformly stable  
 534 algorithms with nearly optimal rate. In *Conference on Learning Theory*, pp. 1270–1279. PMLR,  
 2019.  
 535

536 Dylan J Foster, Spencer Greenberg, Satyen Kale, Haipeng Luo, Mehryar Mohri, and Karthik Sridharan.  
 537 Hypothesis set stability and generalization. *Advances in Neural Information Processing Systems*,  
 538 32, 2019.  
 539

540 Moritz Hardt, Ben Recht, and Yoram Singer. Train faster, generalize better: Stability of stochastic  
 541 gradient descent. In *International conference on machine learning*, pp. 1225–1234. PMLR, 2016.  
 542

540 Hikaru Ibayashi and Masaaki Imaizumi. Exponential escape efficiency of sgd from sharp minima in  
 541 non-stationary regime. *arXiv preprint arXiv:2111.04004*, 2021.  
 542

543 Robert I Jennrich. Asymptotic properties of non-linear least squares estimators. *The Annals of*  
 544 *Mathematical Statistics*, 40(2):633–643, 1969.

545 Nitish Shirish Keskar, Dheevatsa Mudigere, Jorge Nocedal, Mikhail Smelyanskiy, and Ping Tak Peter  
 546 Tang. On large-batch training for deep learning: Generalization gap and sharp minima. *arXiv*  
 547 *preprint arXiv:1609.04836*, 2016.

548

549 Nicolas Loizou, Sharan Vaswani, Issam Hadj Laradji, and Simon Lacoste-Julien. Stochastic polyak  
 550 step-size for sgd: An adaptive learning rate for fast convergence. In *International Conference on*  
 551 *Artificial Intelligence and Statistics*, pp. 1306–1314. PMLR, 2021.

552 Chao Ma and Lexing Ying. On linear stability of sgd and input-smoothness of neural networks.  
 553 *Advances in Neural Information Processing Systems*, 34:16805–16817, 2021.

554

555 Panayotis Mertikopoulos, Nadav Hallak, Ali Kavis, and Volkan Cevher. On the almost sure conver-  
 556 gence of stochastic gradient descent in non-convex problems. *Advances in Neural Information*  
 557 *Processing Systems*, 33:1117–1128, 2020.

558 Scott Pesme, Loucas Pillaud-Vivien, and Nicolas Flammarion. Implicit bias of sgd for diagonal linear  
 559 networks: a provable benefit of stochasticity. *Advances in Neural Information Processing Systems*,  
 560 34:29218–29230, 2021.

561

562 Peter Richtárik and Martin Takáć. Stochastic reformulations of linear systems: algorithms and  
 563 convergence theory. *SIAM Journal on Matrix Analysis and Applications*, 41(2):487–524, 2020.

564

565 Shai Shalev-Shwartz, Ohad Shamir, Nathan Srebro, and Karthik Sridharan. Learnability, stability  
 566 and uniform convergence. *The Journal of Machine Learning Research*, 11:2635–2670, 2010.

567

568 Samuel L Smith, Benoit Dherin, David GT Barrett, and Soham De. On the origin of implicit  
 569 regularization in stochastic gradient descent. *arXiv preprint arXiv:2101.12176*, 2021.

570

571 Valentin Thomas, Fabian Pedregosa, Bart Merriënboer, Pierre-Antoine Manzagol, Yoshua Bengio, and  
 572 Nicolas Le Roux. On the interplay between noise and curvature and its effect on optimization and  
 573 generalization. In *International Conference on Artificial Intelligence and Statistics*, pp. 3503–3513.  
 574 PMLR, 2020.

575

576 Sharan Vaswani, Francis Bach, and Mark Schmidt. Fast and faster convergence of sgd for over-  
 577 parameterized models and an accelerated perceptron. In *The 22nd international conference on*  
 578 *artificial intelligence and statistics*, pp. 1195–1204. PMLR, 2019.

579

580 Lei Wu and Weijie J Su. The implicit regularization of dynamical stability in stochastic gradient  
 581 descent. In *International Conference on Machine Learning*, pp. 37656–37684. PMLR, 2023.

582

583 Lei Wu, Mingze Wang, and Weijie Su. The alignment property of sgd noise and how it helps select flat  
 584 minima: A stability analysis. *Advances in Neural Information Processing Systems*, 35:4680–4693,  
 585 2022.

586

587 Han Xiao, Kashif Rasul, and Roland Vollgraf. Fashion-mnist: a novel image dataset for benchmarking  
 588 machine learning algorithms. *arXiv preprint arXiv:1708.07747*, 2017.

589

590 Ning Yang, Chao Tang, and Yuhai Tu. Stochastic gradient descent introduces an effective landscape-  
 591 dependent regularization favoring flat solutions. *Physical Review Letters*, 130(23):237101, 2023.

592

593 Chiyuan Zhang, Samy Bengio, Moritz Hardt, Benjamin Recht, and Oriol Vinyals. Understanding  
 594 deep learning requires rethinking generalization. *arXiv preprint arXiv:1611.03530*, 2016.

595

596 Yi Zhou, Yingbin Liang, and Huishuai Zhang. Understanding generalization error of sgd in nonconvex  
 597 optimization. *Machine Learning*, pp. 1–31, 2022.

598

599

594 **A EXPERIMENTAL SETUP**595 **A.1 IDEALIZED EXPERIMENT**

598 We consider a set of 30 different candidate functions as the population. Each function has a local  
 599 minimum at  $(7, 7)$ , as well as an additional critical point. This second critical point is located at one  
 600 point drawn uniformly from the set  $\{(1, 1), (1, 4), (1, 7), (4, 1), (4, 4), (4, 7), (7, 1), (7, 4)\}$ . With  
 601 probability  $\rho$ , the additional critical point is a local maximum; otherwise, it is a local minimum. We  
 602 set  $\rho = 0.35$ . Each critical point is modeled by a Gaussian function, with its height and width drawn  
 603 from Gaussian distributions. We construct 10 training sets. Each training set contains 30 candidate  
 604 functions, sampled with replacement from the population. We run all experiments for 200 iterations  
 605 with an initial learning rate of 0.4 and decay rate of 0.99. Each algorithm is evaluated over 100  
 606 different initializations, arranged in a  $10 \times 10$  grid on the domain  $[0, 8] \times [0, 8]$ , and the results are  
 607 averaged.

608 This experiment was conducted on an Apple MacBook Pro equipped with an M1 Pro processor and  
 609 16 GB of memory. The typical running time for a single training set is approximately 19 minutes.

610 **A.2 SPARSE REGRESSION WITH DIAGONAL LINEAR NETWORKS**

612 For each training set and initialization combination, we run experiments with three different model  
 613 initializations and four training sets and average the results to account for the stochasticity. Each training  
 614 set contains 40 samples whose inputs are drawn from a 100-d Gaussian distribution  $\mathcal{N}(0, I_{100})$ .  
 615 The label for each sample is generated by taking the inner product between the true solution vector  $\beta$   
 616 and the input, then adding a Gaussian noise to it:

$$617 \quad 618 \quad y_i = \langle \beta, x_i \rangle + \xi, \xi \sim \mathcal{N}(0, 1). \quad (13)$$

619 The sparse true solution vector  $\beta$  has 5 non-zero entries, randomly generated from a Gaussian  
 620 distribution  $\mathcal{N}(0, 2I_5)$ .

621 For each combination of initialization and training set, we run the algorithms 4 times and take the  
 622 average over the results. We use a constant learning rate of 0.01 throughout the 200 training epochs.

624 Experiments were conducted using NVIDIA V100 GPUs with 32 GB of memory. For both one and  
 625 two explicit regularizers, the typical running time of SGD is approximately 3.2 hours for 200 epochs  
 626 at a given regularization strength.

627 **A.3 DEEP NEURAL NETWORKS**

629 We conduct experiments with only regularizer 2, because it is much more tractable to compute than  
 630 regularizer 1. We omit the batch gradient term  $\nabla L(S; A_{t-1}(S))$  to further reduce the computational  
 631 cost.

633 The CNN has two convolutional layers, whose structures are (in\_channels=1, out\_channels=32,  
 634 kernel\_size=3, stride=1, padding=1) and (in\_channels=32, out\_channels=64, kernel\_size=3, stride=1,  
 635 padding=1), and one fully-connected hidden layer with 128 nodes. We run each algorithm for 400  
 636 epochs with gradient clipping and batch size 32. To accelerate convergence, we let the learning rate  
 637 decay by 1% after each epoch. For the weight decay benchmark, we conduct a grid search over  
 638 candidate values of the decay rate and select 0.01 as the optimal setting.

639 Experiments were conducted using NVIDIA V100 GPUs with 32 GB of memory. The typical running  
 640 times for the original SGD and SGD with the explicit regularizer are 2.5 and 5.5 hours for 400 epochs  
 641 at a given regularization strength.

642 **B PROOFS**643 **B.1 PROOF OF LEMMA 1**

645 **Lemma 1.** Consider a loss function  $L$  whose value is bounded by  $U_L$ , with batch gradient  $\ell_2$ -norm  
 646 bounded by  $U_G$  and all third-order partial derivatives bounded by  $U_J$ . Assume the parameters are

648 bounded as  $\|\theta\|_2 \leq U_F$ . If Assumptions 1 and 2 hold for  $L$ , the expected generalization gap satisfies  
649

$$650 \mathbb{E}_{S, A_T} [L(D; A_T(S)) - L(S; A_T(S))] \quad (1)$$

$$651 = \frac{1}{N} \sum_{i=1}^N \mathbb{E}_{S, z'_i, A_T} [L(z'_i; A_T(S))] - \frac{1}{N} \sum_{i=1}^N \mathbb{E}_{S, z'_i, A_T} [L(z'_i; A_T(S^i))] \quad (2)$$

$$654 = \mathbb{E}_{S, A_T} \left[ \frac{1}{2} \text{Tr} \left( \nabla^2 L(S; A_T(S)) \frac{1}{N} \sum_{i=1}^N \mathbb{E}_{z'_i} [J(A_T(S^i) - A_T(S))] \right) \right] \quad (3)$$

$$657 + \mathcal{O}(\epsilon_{1,T} \epsilon_{2,T} + \delta_{1,T} \epsilon_{2,T} U_G + \delta_{1,T} \delta_{2,T} U_G U_F + \epsilon_{2,T}^3 U_J + \delta_{2,T} U_L). \quad (4)$$

659 *Proof.* As mentioned in the main article,  $\mathbb{E}_{z'_i} [f]$  means  $\mathbb{E}_{z'_i \sim D} [f]$  and  $\mathbb{E}_S [f]$  means  $\mathbb{E}_{S \sim D^N} [f]$ .  
660

661 Note that for a specific realization of SGD, it is no longer symmetric in each sample of the training  
662 set. Intuitively, it makes a bigger difference when the replacement happens earlier rather than later.  
663 So, we will average over all the  $N$  locations in the training set. We write the expected training loss  
664 over  $S$  and  $A_T$  in terms of sample losses:  
665

$$666 \mathbb{E}_{S, A_T} [L(S; A_T(S))] = \mathbb{E}_{A_T} [\mathbb{E}_S [L(S; A_T(S))]] \quad (14)$$

$$667 = \mathbb{E}_{A_T} \left[ \mathbb{E}_S \left[ \frac{1}{N} \sum_{i=1}^N L(z_i; A_T(S)) \right] \right] \quad (15)$$

$$669 = \mathbb{E}_{A_T} \left[ \frac{1}{N} \sum_{i=1}^N \mathbb{E}_S [L(z_i; A_T(S))] \right] \quad (16)$$

$$672 = \frac{1}{N} \sum_{i=1}^N \mathbb{E}_{S, A_T} [L(z_i; A_T(S))]. \quad (17)$$

675 Note that for a certain  $i \in [N]$ ,  $\mathbb{E}_S [L(z_i; A_T(S))] = \mathbb{E}_{S, z'_i} [L(z'_i; A_T(S^i))]$  and thus,  
676

$$678 \mathbb{E}_{S, A_T} [L(S; A_T(S))] = \frac{1}{N} \sum_{i=1}^N \mathbb{E}_{S, z'_i, A_T} [L(z'_i; A_T(S^i))]. \quad (18)$$

681 The expected generalization gap can be formulated as

$$682 \mathbb{E}_{S, A_T} [L(D; A_T(S)) - L(S; A_T(S))] \quad (19)$$

$$684 = \frac{1}{N} \sum_{i=1}^N \mathbb{E}_{S, z'_i, A_T} [L(z'_i; A_T(S))] - \frac{1}{N} \sum_{i=1}^N \mathbb{E}_{S, z'_i, A_T} [L(z'_i; A_T(S^i))] \quad (20)$$

$$687 = \frac{1}{N} \sum_{i=1}^N \mathbb{E}_{S, z'_i, A_T} [L(z'_i; A_T(S)) - L(z'_i; A_T(S^i))]. \quad (21)$$

690 We apply a second-order Taylor expansion to the expression in equation 21:

$$692 = \frac{1}{N} \sum_{i=1}^N \mathbb{E}_{S, z'_i, A_T} [L(z'_i; A_T(S)) - L(z'_i; A_T(S^i))] \quad (22)$$

$$695 = \frac{1}{N} \sum_{i=1}^N \mathbb{E}_{S, z'_i, A_T} \left[ \nabla L(z'_i; A_T(S^i)) (A_T(S) - A_T(S^i)) \right. \quad (23)$$

$$698 \left. + \frac{1}{2} (A_T(S) - A_T(S^i))^T \nabla^2 L(z'_i; A_T(S^i)) (A_T(S) - A_T(S^i)) \right] \quad (24)$$

$$700 + \mathcal{O}(\epsilon_{2,T}^3 U_J + \delta_{2,T} U_L). \quad (25)$$

701 The terms  $\epsilon_{2,T}^3 U_J$  and  $\delta_{2,T} U_L$  constitute the remainder of the second-order Taylor expansion.

702 Recall that Assumption 1 assumes that the gradient  $\ell_2$ -norm,  $\|\nabla L(z'_i; A_T(S^i))\|_2$ , is bounded by  
 703  $\epsilon_{1,T}$  with probability  $1 - \delta_{1,T}$ . Therefore, we can bound the first-order term in equation 22 by  
 704

$$705 \quad \frac{1}{N} \sum_{i=1}^N \mathbb{E}_{S, z'_i, A_T} [\nabla L(z'_i; A_T(S^i)) (A_T(S) - A_T(S^i))] \quad (26)$$

$$706 \quad + \frac{1}{2} (A_T(S) - A_T(S^i))^T \nabla^2 L(z'_i; A_T(S^i)) (A_T(S) - A_T(S^i)) \quad (27)$$

$$707 \quad + \mathcal{O}(\epsilon_{2,T}^3 U_J + \delta_{2,T} U_L) \quad (28)$$

$$708 \quad = \frac{1}{N} \sum_{i=1}^N \mathbb{E}_{S, z'_i, A_T} \left[ \frac{1}{2} (A_T(S) - A_T(S^i))^T \nabla^2 L(z'_i; A_T(S^i)) (A_T(S) - A_T(S^i)) \right] \quad (29)$$

$$709 \quad + \mathcal{O}(\epsilon_{1,T} \epsilon_{2,T} + \delta_{1,T} \epsilon_{2,T} U_G + \delta_{1,T} \delta_{2,T} U_G U_F + \epsilon_{2,T}^3 U_J + \delta_{2,T} U_L) \quad (30)$$

$$710 \quad = \frac{1}{N} \sum_{i=1}^N \mathbb{E}_{S, z'_i, A_T} \left[ \frac{1}{2} \text{Tr}(\nabla^2 L(z'_i; A_T(S^i)) J(A_T(S) - A_T(S^i))) \right] \quad (31)$$

$$711 \quad + \mathcal{O}(\epsilon_{1,T} \epsilon_{2,T} + \delta_{1,T} \epsilon_{2,T} U_G + \delta_{1,T} \delta_{2,T} U_G U_F + \epsilon_{2,T}^3 U_J + \delta_{2,T} U_L). \quad (32)$$

721 The term  $\epsilon_{1,T} \epsilon_{2,T}$  corresponds to the case where both Assumption 1 and 2 hold, the term  $\delta_{1,T} \epsilon_{2,T} U_G$   
 722 corresponds to the case where Assumption 1 does not hold but Assumption 2 holds, and the term  
 723  $\delta_{1,T} \delta_{2,T} U_G U_F$  corresponds to the case where neither of the two assumptions holds. The term  
 724 corresponding to the case where Assumption 1 holds but Assumption 2 does not hold is dominated  
 725 by  $\delta_{2,T} U_L$ .

726 Because sampling  $(S, z'_i)$  and  $(S^i, z_i)$  are symmetric,

$$727 \quad \mathbb{E}_{S, z'_i, A_T} [f(S, S^i, z_i, z'_i, A_T)] = \mathbb{E}_{S^i, z_i, A_T} [f(S, S^i, z_i, z'_i, A_T)]$$

731 for any function  $f$ . Therefore, we can exchange  $z_i$  with  $z'_i$  and  $S$  with  $S^i$  in equation 31, and then  
 732 apply the bound on the solution deviation in Assumption 2 to obtain  
 733

$$734 \quad \frac{1}{N} \sum_{i=1}^N \mathbb{E}_{S, z'_i, A_T} \left[ \frac{1}{2} \text{Tr}(\nabla^2 L(z'_i; A_T(S^i)) J(A_T(S) - A_T(S^i))) \right] \quad (33)$$

$$735 \quad = \frac{1}{N} \sum_{i=1}^N \mathbb{E}_{S^i, z_i, A_T} \left[ \frac{1}{2} \text{Tr}(\nabla^2 L(z'_i; A_T(S^i)) J(A_T(S) - A_T(S^i))) \right] \quad (34)$$

$$736 \quad = \frac{1}{N} \sum_{i=1}^N \mathbb{E}_{S, z'_i, A_T} \left[ \frac{1}{2} \text{Tr}(\nabla^2 L(z_i; A_T(S)) J(A_T(S^i) - A_T(S))) \right] \quad (35)$$

$$737 \quad = \frac{1}{N} \sum_{i=1}^N \mathbb{E}_{S, A_T} \left[ \frac{1}{2} \text{Tr}(\nabla^2 L(z_i; A_T(S)) \frac{1}{N} \sum_{q=1}^N \mathbb{E}_{z'_q} [J(A_T(S^q) - A_T(S))] \right] \quad (36)$$

$$738 \quad + \mathcal{O}(\epsilon_{2,T}^3 U_J + \delta_{2,T} U_L) \quad (37)$$

$$739 \quad = \mathbb{E}_{S, z'_i, A_T} \left[ \frac{1}{2} \text{Tr} \left( \frac{1}{N} \sum_{i=1}^N \nabla^2 L(z_i; A_T(S)) \frac{1}{N} \sum_{q=1}^N \mathbb{E}_{z'_q} [J(A_T(S^i) - A_T(S))] \right) \right] \quad (38)$$

$$740 \quad + \mathcal{O}(\epsilon_{2,T}^3 U_J + \delta_{2,T} U_L) \quad (39)$$

$$741 \quad = \mathbb{E}_{S, A_T} \left[ \frac{1}{2} \text{Tr} \left( \nabla^2 L(S; A_T(S)) \frac{1}{N} \sum_{i=1}^N \mathbb{E}_{z'_i} [J(A_T(S^i) - A_T(S))] \right) \right] \quad (40)$$

$$742 \quad + \mathcal{O}(\epsilon_{2,T}^3 U_J + \delta_{2,T} U_L). \quad (41)$$

756 Plugging equation 40-equation 41 into equation 31 gives the desired result:  
757

$$758 \mathbb{E}_{S, A_T} [L(D; A_T(S)) - L(S; A_T(S))] \quad (42)$$

$$759 = \mathbb{E}_{S, A_T} \left[ \frac{1}{2} \text{Tr} \left( \nabla^2 L(S; A_T(S)) \frac{1}{N} \sum_{i=1}^N \mathbb{E}_{z'_i} [J(A_T(S^i) - A_T(S))] \right) \right] \quad (43)$$

$$762 + \mathcal{O}(\epsilon_{1,T} \epsilon_{2,T} + \delta_{1,T} \epsilon_{2,T} U_G + \delta_{1,T} \delta_{2,T} U_G U_F + \epsilon_{2,T}^3 U_J + \delta_{2,T} U_L). \quad (44)$$

763  $\square$   
764

## 765 B.2 PROOF OF LEMMA 2

767 **Lemma 2.** Consider the case where the model is trained with SGD on the training set  $S$  for  $M$   
768 epochs, with each sample appearing exactly once in every epoch. Assume that  
769

- 770 1. The learning rates are small, i.e., letting  $Q = \max_t \eta_t$ , we have  $Q \ll 1$ .
- 771 2. The operator norm of  $\nabla^2 L(S; \theta)$  is uniformly bounded by a constant  $C \ll \frac{1}{Q}$ .

773 Then, the algorithmic variability can be bounded as  
774

$$775 \text{Tr} \left( \nabla^2 L(S, A_T(S)) \frac{1}{N} \sum_{i=1}^N \mathbb{E}_{z'_i} [J(A_T(S^i) - A_T(S))] \right) \quad (5)$$

$$778 \leq \text{Tr} \left( \nabla^2 L(S, A_T(S)) \sum_{t=1}^T M \eta_t^2 \mathbb{E}_{z'_i} [J(\nabla L(z'_i; A_{t-1}(S)) - \nabla L(D; A_{t-1}(S)))] \right) \quad (6)$$

$$781 + \text{Tr} \left( \nabla^2 L(S, A_T(S)) \sum_{t=1}^T M \eta_t^2 J(\nabla L(S_{j_t}; A_{t-1}(S)) - \nabla L(D; A_{t-1}(S))) \right) \quad (7)$$

$$784 + \mathcal{O}(T Q \epsilon_{2,T} (\epsilon_{2,T}^3 U_J + \delta_{2,T} U_L U_F^3 + C Q U_F) + T^2 Q^2 (\epsilon_{2,T}^3 U_J + \delta_{2,T} U_L U_F^3 + C Q U_F)^2). \quad (8)$$

787 *Proof.* For simplicity of exposition, and without loss of generality, we only consider the case of SGD  
788 with batch size 1 in this proof.

789 From a fixed model initialization  $A_0$ , the update rule of SGD leads to  
790

$$791 A_T(S) = A_0 - \sum_{t=1}^T \eta_t \nabla L(S_{j_t}; A_{t-1}(S)) \quad (45)$$

794 and  
795

$$796 A_T(S^i) = A_0 - \sum_{t=1}^T \eta_t \nabla L(S_{j_t}^i; A_{t-1}(S^i)). \quad (46)$$

799 Thus,  
800

$$801 A_T(S^i) - A_T(S) = \sum_{t=1}^T \eta_t (\nabla L(S_{j_t}; A_{t-1}(S)) - \nabla L(S_{j_t}^i; A_{t-1}(S^i))). \quad (47)$$

803 Now we prove by induction that  
804

$$805 A_k(S^i) - A_k(S) = \sum_{t=1}^k \eta_t (\nabla L(S_{j_t}; A_{t-1}(S)) - \nabla L(S_{j_t}^i; A_{t-1}(S))) \quad (48)$$

$$808 + \mathcal{O}(k Q (\epsilon_{2,T}^3 U_J + \delta_{2,T} U_L U_F^3 + C Q U_F)), \quad (49)$$

809 for  $k = [T]$ .

810 Base case: Because  $A_0(S) = A_0(S^i) = A_0$ , it is easy to check that equation 48-equation 49 hold  
811 when  $k = 1$ .

812 Inductive hypothesis: Suppose equation 48-equation 49 hold for all  $1 \leq k \leq p$ .

813 Inductive step:

$$814 \quad A_{p+1}(S^i) - A_{p+1}(S) \quad (50)$$

$$815 \quad = A_p(S^i) - A_p(S) - \eta_{p+1} \nabla L(S_{j_{p+1}}^i; A_p(S^i)) + \eta_{p+1} \nabla L(S_{j_{p+1}}; A_p(S)) \quad (51)$$

$$816 \quad = A_p(S^i) - A_p(S) + \eta_{p+1} \left( \nabla L(S_{j_{p+1}}; A_p(S)) - \nabla L(S_{j_{p+1}}^i; A_p(S)) \right) \quad (52)$$

$$817 \quad - \eta_{p+1} \left( \nabla L(S_{j_{p+1}}^i; A_p(S^i)) - \nabla L(S_{j_{p+1}}^i; A_p(S)) \right). \quad (53)$$

818 The solution stability bound grows with the number of iterations (Hardt et al., 2016). Consequently,  
819 Assumption 2 holds with  $\epsilon_{2,T}$  and  $\delta_{2,T}$  for the entire training process. We can apply a Taylor  
820 expansion to the term in equation 53:

$$821 \quad \nabla L(S_{j_{p+1}}^i; A_p(S^i)) - \nabla L(S_{j_{p+1}}^i; A_p(S)) \quad (54)$$

$$822 \quad = \nabla^2 L(S_{j_{p+1}}^i; A_p(S)) (A_p(S^i) - A_p(S)) + \mathcal{O}(\epsilon_{2,T}^3 U_J + \delta_{2,T} U_L U_F^3). \quad (55)$$

823 Recall that the Hessian operator norm is bounded by  $C \ll \frac{1}{Q}$ . Plugging equation 55 back into  
824 equation 53 obtains

$$825 \quad A_{p+1}(S^i) - A_{p+1}(S) \quad (56)$$

$$826 \quad = A_p(S^i) - A_p(S) + \eta_{p+1} \left( \nabla L(S_{j_{p+1}}; A_p(S)) - \nabla L(S_{j_{p+1}}^i; A_p(S)) \right) \quad (57)$$

$$827 \quad - \eta_{p+1} \left( \nabla L(S_{j_{p+1}}^i; A_p(S^i)) - \nabla L(S_{j_{p+1}}^i; A_p(S)) \right) \quad (58)$$

$$828 \quad = A_p(S^i) - A_p(S) + \eta_{p+1} \left( \nabla L(S_{j_{p+1}}; A_p(S)) - \nabla L(S_{j_{p+1}}^i; A_p(S)) \right) \quad (59)$$

$$829 \quad - \eta_{p+1} \nabla^2 L(S_{j_{p+1}}^i; A_p(S)) (A_p(S^i) - A_p(S)) + \mathcal{O}(Q(\epsilon_{2,T}^3 U_J + \delta_{2,T} U_L U_F^3)) \quad (60)$$

$$830 \quad = A_p(S^i) - A_p(S) + \eta_{p+1} \left( \nabla L(S_{j_{p+1}}; A_p(S)) - \nabla L(S_{j_{p+1}}^i; A_p(S)) \right) \quad (61)$$

$$831 \quad + \mathcal{O}(Q(\epsilon_{2,T}^3 U_J + \delta_{2,T} U_L U_F^3 + C Q U_F)) \quad (62)$$

$$832 \quad = \sum_{t=1}^p \eta_t \left( \nabla L(S_{j_t}; A_{t-1}(S)) - \nabla L(S_{j_t}^i; A_{t-1}(S)) \right) \quad (63)$$

$$833 \quad + \mathcal{O}(p Q (\epsilon_{2,T}^3 U_J + \delta_{2,T} U_L U_F^3 + C Q U_F)) \quad (64)$$

$$834 \quad + \eta_{p+1} \left( \nabla L(S_{j_{p+1}}; A_p(S)) - \nabla L(S_{j_{p+1}}^i; A_p(S)) \right) \quad (65)$$

$$835 \quad + \mathcal{O}(Q(\epsilon_{2,T}^3 U_J + \delta_{2,T} U_L U_F^3 + C Q U_F)) \quad (66)$$

$$836 \quad = \sum_{t=1}^{p+1} \eta_t \left( \nabla L(S_{j_t}; A_{t-1}(S)) - \nabla L(S_{j_t}^i; A_{t-1}(S)) \right) \quad (67)$$

$$837 \quad + \mathcal{O}((p+1) Q (\epsilon_{2,T}^3 U_J + \delta_{2,T} U_L U_F^3 + C Q U_F)). \quad (68)$$

838 Thus, equation 48-equation 49 also hold for the case  $k = p + 1$ . By the principle of mathematical  
839 induction,

$$840 \quad A_k(S^i) - A_k(S) = \sum_{t=1}^k \eta_t \left( \nabla L(S_{j_t}; A_{t-1}(S)) - \nabla L(S_{j_t}^i; A_{t-1}(S)) \right) \quad (69)$$

$$841 \quad + \mathcal{O}(k Q (\epsilon_{2,T}^3 U_J + \delta_{2,T} U_L U_F^3 + C Q U_F)) \quad (70)$$

864 for  $k = [T]$ .  
865

866 For each  $i \in [N]$ , there are  $M$  indices  $t$  such that  $j_t = i$ . For simplicity of notation, we require that  
867 the sample sequence is not shuffled for different epochs, so that  $j_m = j_{m+rN} = m, m \in [N], r \in$   
868  $[M - 1]$ . However, the result also holds when the sample sequence is shuffled in each epoch.

869 It follows that

$$870 \text{Tr} \left( \nabla^2 L(S, A_T(S)) \frac{1}{N} \sum_{i=1}^N \mathbb{E}_{z'_i} [J(A_T(S^i) - A_T(S))] \right) \quad (71)$$

$$873 = \text{Tr} \left( \nabla^2 L(S, A_T(S)) \frac{1}{N} \sum_{i=1}^N \mathbb{E}_{z'_i} \left[ J \left( \sum_{t=1}^T \eta_t (\nabla L(S_{j_t}; A_{t-1}(S)) - \nabla L(S_{j_t}^i; A_{t-1}(S))) \right) \right] \right) \quad (72)$$

$$877 + \mathcal{O} \left( T Q \epsilon_{2,T} (\epsilon_{2,T}^3 U_J + \delta_{2,T} U_L U_F^3 + C Q U_F) + T^2 Q^2 (\epsilon_{2,T}^3 U_J + \delta_{2,T} U_L U_F^3 + C Q U_F)^2 \right). \quad (73)$$

880 Note that

$$881 \sum_{i=1}^N \mathbb{E}_{z'_i} [(\nabla L(S_{j_m}; A_{m-1}(S)) - \nabla L(S_{j_m}^i; A_{m-1}(S))) \quad (74)$$

$$884 (\nabla L(S_{j_n}; A_{n-1}(S)) - \nabla L(S_{j_n}^i; A_{n-1}(S)))^T] = 0 \quad (75)$$

885 when  $j_m \neq j_n$ . In this case, since  $S$  and  $S^i$  only differ in the  $i$ -th sample, either  $S_{j_m} = S_{j_m}^i$  or  
886  $S_{j_n} = S_{j_n}^i$ , making the outer product of the gradient differences zero. Hence,

$$888 \text{Tr} \left( \nabla^2 L(S, A_T(S)) \frac{1}{N} \sum_{i=1}^N \mathbb{E}_{z'_i} \left[ J \left( \sum_{t=1}^T \eta_t (\nabla L(S_{j_t}; A_{t-1}(S)) - \nabla L(S_{j_t}^i; A_{t-1}(S))) \right) \right] \right) \quad (76)$$

$$892 = \text{Tr} \left( \nabla^2 L(S, A_T(S)) \quad (77)$$

$$895 \sum_{i=1}^N \mathbb{E}_{z'_i} \left[ J \left( \sum_{r=0}^{M-1} \eta_{i+rN} (\nabla L(S_{j_{i+rN}}; A_{i+rN-1}(S)) - \nabla L(S_{j_{i+rN}}^i; A_{i+rN-1}(S))) \right) \right] \quad (78)$$

$$899 \leq \text{Tr} \left( \nabla^2 L(S, A_T(S)) \quad (79)$$

$$902 \sum_{i=1}^N \mathbb{E}_{z'_i} \left[ \sum_{r=0}^{M-1} M \eta_{i+rN}^2 J (\nabla L(S_{j_{i+rN}}; A_{i+rN-1}(S)) - \nabla L(S_{j_{i+rN}}^i; A_{i+rN-1}(S))) \right] \quad (80)$$

$$905 = \text{Tr} \left( \nabla^2 L(S, A_T(S)) \sum_{t=1}^T M \eta_t^2 \mathbb{E}_{z'_{j_t} \sim D} \left[ J (\nabla L(S_{j_t}; A_{t-1}(S)) - \nabla L(S_{j_t}^i; A_{t-1}(S))) \right] \right) \quad (81)$$

$$910 = \text{Tr} \left( \nabla^2 L(S, A_T(S)) \sum_{t=1}^T M \eta_t^2 \mathbb{E}_{z'_{j_t} \sim D} \left[ J (\nabla L(S_{j_t}; A_{t-1}(S)) - \nabla L(z'_{j_t}; A_{t-1}(S))) \right] \right) \quad (82)$$

$$914 = \text{Tr} \left( \nabla^2 L(S, A_T(S)) \sum_{t=1}^T M \eta_t^2 \mathbb{E}_{z'_i} \left[ J (\nabla L(S_{j_t}; A_{t-1}(S)) - \nabla L(z'_i; A_{t-1}(S))) \right] \right) \quad (83)$$

$$917 = \text{Tr} \left( \nabla^2 L(S, A_T(S)) \mathbb{E}_{z'_i} \left[ \sum_{t=1}^T M \eta_t^2 J (\nabla L(S_{j_t}; A_{t-1}(S)) - \nabla L(z'_i; A_{t-1}(S))) \right] \right). \quad (84)$$

918 Equation 77-equation 78 aggregate all iterations which select the same samples in the  $\sum_{r=0}^{M-1}$  sum,  
 919 and the factor  $\frac{1}{N}$  is absent because there is exactly one  $i$  for which this expectation is non-zero. The  
 920 inequality in equation 79-equation 80 results from the fact that, for any positive semi-definite matrix  
 921  $G \in \mathbb{R}^{d \times d}$  and any vector sequence  $\{u_p \in \mathbb{R}^d : p \in [M]\}$ ,

$$923 \quad \text{Tr} \left( G J \left( \sum_{p=1}^M u_p \right) \right) \leq \text{Tr} \left( G M \sum_{p=1}^M J(u_p) \right), \quad (85)$$

926 which can be derived as follows:

$$928 \quad \text{Tr} \left( G M \sum_{p=1}^M J(u_p) \right) - \text{Tr} \left( G J \left( \sum_{p=1}^M u_p \right) \right) \quad (86)$$

$$931 \quad = M \sum_{p=1}^M \|u_p\|_G^2 - \left\| \sum_{p=1}^M u_p \right\|_G^2 \quad (87)$$

$$935 \quad = \frac{1}{2} \sum_{p,q=1, p \neq q}^M \|u_p - u_q\|_G^2 \quad (88)$$

$$938 \quad \geq 0. \quad (89)$$

939 By plugging the results in equation 76-equation 84 into equation 71-equation 73 and rearranging the  
 940 terms, we obtain

$$942 \quad \text{Tr} \left( \nabla^2 L(S, A_T(S)) \frac{1}{N} \sum_{i=1}^N \mathbb{E}_{z'_i} [J(A_T(S^i) - A_T(S))] \right) \quad (90)$$

$$945 \quad \leq \text{Tr} \left( \nabla^2 L(S, A_T(S)) \mathbb{E}_{z'_i} \left[ \sum_{t=1}^T M \eta_t^2 J(\nabla L(S_{j_t}; A_{t-1}(S)) - \nabla L(z'_i; A_{t-1}(S))) \right] \right) \quad (91)$$

$$948 \quad + \mathcal{O} \left( T Q \epsilon_{2,T} (\epsilon_{2,T}^3 U_J + \delta_{2,T} U_L U_F^3 + C Q U_F) + T^2 Q^2 (\epsilon_{2,T}^3 U_J + \delta_{2,T} U_L U_F^3 + C Q U_F)^2 \right) \quad (92)$$

$$951 \quad = \text{Tr} \left( \nabla^2 L(S, A_T(S)) \mathbb{E}_{z'_i} \left[ \sum_{t=1}^T M \eta_t^2 J \left( (\nabla L(S_{j_t}; A_{t-1}(S)) - \nabla L(D; A_{t-1}(S))) \right. \right. \right. \quad (93)$$

$$954 \quad \left. \left. \left. + (\nabla L(D; A_{t-1}(S)) - \nabla L(z'_i; A_{t-1}(S))) \right) \right] \right) \quad (94)$$

$$956 \quad + \mathcal{O} \left( T Q \epsilon_{2,T} (\epsilon_{2,T}^3 U_J + \delta_{2,T} U_L U_F^3 + C Q U_F) + T^2 Q^2 (\epsilon_{2,T}^3 U_J + \delta_{2,T} U_L U_F^3 + C Q U_F)^2 \right). \quad (95)$$

959 Note that

$$962 \quad \mathbb{E}_{z'_i} \left[ (\nabla L(S_{j_t}; A_{t-1}(S)) - \nabla L(D; A_{t-1}(S))) (\nabla L(D; A_{t-1}(S)) - \nabla L(z'_i; A_{t-1}(S)))^T \right] \quad (96)$$

$$965 \quad = (\nabla L(S_{j_t}; A_{t-1}(S)) - \nabla L(D; A_{t-1}(S))) \mathbb{E}_{z'_i} \left[ (\nabla L(D; A_{t-1}(S)) - \nabla L(z'_i; A_{t-1}(S)))^T \right] \quad (97)$$

$$968 \quad = (\nabla L(S_{j_t}; A_{t-1}(S)) - \nabla L(D; A_{t-1}(S))) (\nabla L(D; A_{t-1}(S)) - \mathbb{E}_{z'_i} [\nabla L(z'_i; A_{t-1}(S))])^T \quad (98)$$

$$970 \quad = (\nabla L(S_{j_t}; A_{t-1}(S)) - \nabla L(D; A_{t-1}(S))) (\nabla L(D; A_{t-1}(S)) - \nabla L(D; A_{t-1}(S)))^T \quad (99)$$

$$971 \quad = 0. \quad (100)$$

972 Plugging this identity back into equation 93-equation 94 yields the desired result:  
 973

974

$$975 \text{Tr} \left( \nabla^2 L(S, A_T(S)) \frac{1}{N} \sum_{i=1}^N \mathbb{E}_{z'_i} [J(A_T(S^i) - A_T(S))] \right) \quad (101)$$

976

977

$$978 \leq \text{Tr} \left( \nabla^2 L(S, A_T(S)) \mathbb{E}_{z'_i} \left[ \sum_{t=1}^T M \eta_t^2 J \left( (\nabla L(S_{j_t}; A_{t-1}(S)) - \nabla L(D; A_{t-1}(S))) \right. \right. \right. \quad (102)$$

979

980

$$981 \quad \left. \left. \left. + (\nabla L(D; A_{t-1}(S)) - \nabla L(z'_i; A_{t-1}(S))) \right) \right] \right) \quad (103)$$

982

983

$$984 + \mathcal{O} \left( T Q \epsilon_{2,T} (\epsilon_{2,T}^3 U_J + \delta_{2,T} U_L U_F^3 + C Q U_F) + T^2 Q^2 (\epsilon_{2,T}^3 U_J + \delta_{2,T} U_L U_F^3 + C Q U_F)^2 \right) \quad (104)$$

985

986

$$987 = \text{Tr} \left( \nabla^2 L(S, A_T(S)) \sum_{t=1}^T M \eta_t^2 \mathbb{E}_{z'_i} [J(\nabla L(D; A_{t-1}(S)) - \nabla L(z'_i; A_{t-1}(S)))] \right) \quad (105)$$

988

989

$$990 + \text{Tr} \left( \nabla^2 L(S, A_T(S)) \sum_{t=1}^T M \eta_t^2 J(\nabla L(S_{j_t}; A_{t-1}(S)) - \nabla L(D; A_{t-1}(S))) \right) \quad (106)$$

991

992

$$993 + \mathcal{O} \left( T Q \epsilon_{2,T} (\epsilon_{2,T}^3 U_J + \delta_{2,T} U_L U_F^3 + C Q U_F) + T^2 Q^2 (\epsilon_{2,T}^3 U_J + \delta_{2,T} U_L U_F^3 + C Q U_F)^2 \right). \quad (107)$$

994

1000 B.3 PROOF OF THEOREM 1

1001

1002 **Theorem 1.** Denote by  $\Sigma_B^S(\theta)$  the gradient covariance of mini-batches of size  $B$  evaluated on  
 1003 dataset  $S$  at  $\theta$ . If the conditions of Lemma 2 hold,  $\theta$  lies within a compact set  $\Theta$ , and  $\nabla L(z'_i; \theta)$   
 1004 is continuous with respect to  $\theta$  on  $\Theta$ , then as the training set size  $N \rightarrow \infty$ , the difference between  
 1005 the accumulated population gradient covariance and the accumulated gradient covariance of SGD  
 1006 converges to 0 almost surely, i.e.,

1007

$$1008 \sum_{t=1}^T \mathbb{E}_{z'_i} [J(\nabla L(z'_i; A_{t-1}(S)) - \nabla L(D; A_{t-1}(S)))] - \sum_{t=1}^T B \Sigma_B^S(A_{t-1}(S)) \xrightarrow{a.s.} 0. \quad (9)$$

1009

1010

1011

1012

1013

1014

1015 *Proof.* We denote a training set of size  $N$  as  $S = \{z_1, z_2, \dots, z_N\}$ ,  $z_i \sim D, i \in [N]$ . We use  $z_i$   
 1016 to denote samples in  $S$ , and  $z'$  to denote an independent sample drawn from either the population  
 1017 distribution  $D$  or the empirical distribution  $D_{emp}^S$  associated with  $S$ . We proceed to define the  
 1018 variables

1019

1020

$$1021 Z_i(\theta) = \nabla L(z_i; \theta) - \nabla L(D; \theta), \quad z_i \sim D, \quad i \in [N] \quad (108)$$

1022

1023

$$1024 \Sigma^D(\theta) = \mathbb{E}_{z' \sim D} [J(\nabla L(z'; \theta) - \nabla L(D; \theta))] \quad (109)$$

1025

1026

$$1027 \bar{Z}_N(\theta) = \frac{1}{N} \sum_{i=1}^N Z_i(\theta). \quad (110)$$

1028

1026 Then, we can write  
 1027

$$1028 \mathbb{E}_{z' \sim D_{emp}^S} \left[ J(\nabla L(z'; \theta) - \nabla L(S; \theta)) \right] \quad (111)$$

$$1030 = \mathbb{E}_{z' \sim D_{emp}^S} \left[ J(\nabla L(z'; \theta) - \nabla L(D; \theta) + \nabla L(D; \theta) - \nabla L(S; \theta)) \right] \quad (112)$$

$$1031 = \mathbb{E}_{z' \sim D_{emp}^S} \left[ J((\nabla L(z'; \theta) - \nabla L(D; \theta)) - (\nabla L(S; \theta) - \nabla L(D; \theta))) \right] \quad (113)$$

$$1033 = \mathbb{E}_{z' \sim D_{emp}^S} \left[ J(\nabla L(z'; \theta) - \nabla L(D; \theta)) \right] - \mathbb{E}_{z' \sim D_{emp}^S} \left[ J(\nabla L(D; \theta) - \nabla L(S; \theta)) \right] \quad (114)$$

$$1035 = \frac{1}{N} \sum_{i=1}^N J(Z_i(\theta)) - J(\bar{Z}_N(\theta)). \quad (115)$$

1038 Let  $v^{(j)}$  indicate the  $j$ -th entry of vector  $v$ . Due to the continuity of  $\nabla L(z'; \theta)$ ,  $Z_i^{(j)}(\theta)$  is a continuous  
 1039 function of  $\theta$  for any  $z_i$ . Also, from the bound on the  $\ell_2$ -norm of the gradient,  $Z_i^{(j)}(\theta)$  is bounded  
 1040 by a function  $h(z_i)$  for any  $z_i$  and  $\theta$ , where  $h$  is an integrable function of  $z_i$  with respect to the  
 1041 distribution  $D$ . With these conditions, according to Theorem 2 in Jennrich (1969), for any  $j, k \in [N]$ ,  
 1042

$$1044 \frac{1}{N} \sum_{i=1}^N Z_i^{(j)}(\theta) Z_i^{(k)}(\theta) \xrightarrow{a.s.} \mathbb{E}_{z_1 \sim D} \left[ Z_1^{(j)}(\theta) Z_1^{(k)}(\theta) \right] = \Sigma_{jk}^D(\theta) \quad (116)$$

1046 uniformly for all  $\theta \in \Theta$  as  $N \rightarrow \infty$ . Because  $Z_i$  has a finite number of entries,

$$1049 \frac{1}{N} \sum_{i=1}^N J(Z_i(\theta)) \xrightarrow{a.s.} \Sigma^D(\theta) \quad (117)$$

1051 uniformly for all  $\theta \in \Theta$  as  $N \rightarrow \infty$ .

1053 From the strong law of large numbers, as the training set size approaches infinity, the mean of any  
 1054 gradient entry over the training set converges almost surely to its population mean. Since  $\bar{Z}_N^{(j)}(\theta)$   
 1055 represents the difference between the mean gradient over the training set  $S$  and the population  
 1056 gradient, for any  $j \in [N]$ ,

$$1057 \bar{Z}_N^{(j)}(\theta) \xrightarrow{a.s.} 0 \quad (118)$$

1059 uniformly for all  $\theta \in \Theta$  as  $N \rightarrow \infty$ . Because  $\bar{Z}_N$  has a finite number of entries,

$$1061 J(\bar{Z}_N(\theta)) \xrightarrow{a.s.} 0 \quad (119)$$

1062 uniformly for all  $\theta \in \Theta$  as  $N \rightarrow \infty$ .

1064 Combining equation 117 and equation 119 leads to

$$1065 \mathbb{E}_{z' \sim D_{emp}^S} \left[ J(\nabla L(z'; \theta) - \nabla L(S; \theta)) \right] - \Sigma^D(\theta) \xrightarrow{a.s.} 0 \quad (120)$$

1067 uniformly for any  $\theta \in \Theta$  as  $N \rightarrow \infty$ .

1069 At  $\theta$ , the gradient covariance of the mini-batches of size  $B$  sampled from dataset  $S$  can be expressed  
 1070 as the empirical gradient covariance  $\Sigma_B^S(\theta) = \frac{1}{B} \mathbb{E}_{z' \sim D_{emp}^S} \left[ J(\nabla L(z'; \theta) - \nabla L(S; \theta)) \right]$ . Thus,  
 1071 with the uniform convergence in equation 120, we obtain

$$1073 \sum_{t=1}^T \mathbb{E}_{z' \sim D} \left[ J(\nabla L(z'; A_{t-1}(S)) - \nabla L(D; A_{t-1}(S))) \right] - \sum_{t=1}^T B \Sigma_B^S(A_{t-1}(S)) \xrightarrow{a.s.} 0 \quad (121)$$

1076 as  $N \rightarrow \infty$ , which is equivalent to the desired result.  $\square$

1077

1078

1079